

# Tails of the dynamical structure factor of 1D spinless fermions beyond the Tomonaga-Luttinger approximation

Sofian Teber\*

Abdus Salam ICTP, Strada Costiera 11, 34014, Trieste, Italy

(Dated: October 16, 2019)

We consider one-dimensional interacting spinless fermions with a non-linear spectrum in a clean quantum wire (non-linear bosonization). We compute diagrammatically the one-dimensional dynamical structure factor,  $S(\omega, q)$ , beyond the Tomonaga-Luttinger approximation focusing on its tails, *i.e.*  $|\omega| \gg vq$ . We provide a re-derivation, through diagrammatics, of the result of Pustilnik, Mishchenko, Glazman, and Andreev [Phys. Rev. Lett. **91**, 126805 (2003)]. We also extend their results to finite temperatures and long-range interactions. As applications we determine curvature and interaction corrections to the small-momentum, high-frequency conductivity and the electron-electron scattering rate.

In the Tomonaga-Luttinger (TL) approximation the single particle fermionic spectrum,  $\xi_k$ , is linear in momentum ( $\xi_k^\pm = \pm vk$  where  $\pm$  correspond to the chirality of the fermions:  $+$  for right-movers and  $-$  for left-movers). As a consequence, excitations are of collective nature, *i.e.* plasmons of velocity  $v$ . This is reflected in the expression for the polarization operator, which reads:

$$\begin{aligned}\Pi_\pm^0(i\omega, q) &= \pm \frac{1}{2\pi} \frac{q}{i\omega \mp vq} \\ \Pi^0(i\omega, q) &= \frac{1}{\pi v} \frac{(vq)^2}{(i\omega)^2 - (vq)^2},\end{aligned}\quad (1)$$

where  $\Pi^0(i\omega, q) = \Pi_+^0(i\omega, q) + \Pi_-^0(i\omega, q)$ . The imaginary part of the retarded polarization operator defines the dynamical structure factor (DSF):

$$S(\omega, q) = -\Im \Pi^R(\omega, q) = -\Im \Pi_+^R(\omega, q) - \Im \Pi_-^R(\omega, q). \quad (2)$$

For non-interacting fermions in the linear spectrum approximation, Eqs. (1) and (2) yield:

$$S^0(\omega, q) = \frac{1}{v} (vq)^2 \delta[\omega^2 - (vq)^2], \quad (3)$$

which is a delta function centered around the mass-shells  $\omega = \pm vq$  of right and left movers. This result implies that the plasmons, or Luttinger bosons, have an infinite life-time and are free. Diagrammatically, *i.e.* as a consequence of the loop cancellation theorem, this fermionic loop with two external lines is the only non-zero one, *i.e.* the sum of all loops with 3 or more external lines is zero, *cf.* Ward identities due to Dzyaloshinskii and Larkin [1] which imply that the RPA is exact. Interactions therefore do not affect the coherent states to all orders. In other words, in any order in the interaction among the fermions the latter may be mapped exactly to a system of free bosons which is the essence of the (non-perturbative in interactions) bosonization technique.

Many contemporary problems require going beyond the Tomonaga-Luttinger approximation. This amounts to consider fermions with a curved spectrum, *i.e.* bare fermionic Green's functions of the form:

$$G_\pm^0(i\epsilon, k) = \frac{1}{i\epsilon - \xi_k^\pm}, \quad \xi_k^\pm = \pm vk + \frac{k^2}{2m}.$$

The academic problem of non-linear bosonization probably dates back to the times of Dzyaloshinskii and Larkin and, since then, has attracted increasing attention both in the field of the solid-state especially during the last decade or so, *e.g.* see Refs. [2,3,4,5,6] without being extensive, and in high-energy physics, see Ref. [7] and references therein. In solid-state physics its importance with respect to small-momentum drag resistivity between quantum wires has been put forward [5] during the last couple of years. Despite its clear relevancy to physical applications, following Ref. [5], there is no rigorous computation of a standard object such as the dynamical structure factor of one-dimensional fermions with curvature *and* interactions. In the absence of interactions the situation is again simple and worth examining. The free-fermion polarization operator (at  $T = 0$ ) with curvature reads:

$$\Pi^0(i\omega, q) = \frac{m}{2\pi q} \ln \left[ \frac{i\omega - vq + q^2/2m}{i\omega - vq - q^2/2m} \right] \quad (4a)$$

$$\begin{aligned}&+ \{i\omega \rightarrow -i\omega, \quad q \rightarrow q\}, \\ S^0(\omega, q) &= -\frac{m}{2|q|} \left[ \theta \left[ -\frac{mv}{q} (\omega - vq + q^2/2m) \right] \right. \\ &\quad \left. - \theta \left[ -\frac{mv}{q} (\omega - vq - q^2/2m) \right] \right] \\ &- \{ \omega \rightarrow -\omega, \quad q \rightarrow q \},\end{aligned}\quad (4b)$$

Notice that at non-zero temperatures the Heaviside functions  $\theta(x)$ , in Eq. (4b), become the Fermi occupation functions  $n_F(x)$ . Eq. (4b) shows explicitly that the DSF satisfies [8]:  $S(\omega, q) = -S(-\omega, q)$ ,  $S(\omega, q) = S(\omega, -q)$ , together with the sum-rule:

$$\int_0^\infty d\omega \omega S(\omega, q) = \bar{n} \frac{q^2}{2m}, \quad (5)$$

where  $\bar{n}$  is the average fermionic density along the wire. Curvature of the spectrum resulting from a finite mass,  $m$ , broadens the delta-function singularities and leads to a decay of the coherent excitations into particle-hole pairs in the range of frequencies delimited by:

$$\omega_- = \pm vq - q^2/2m < \omega < \omega_+ = \pm vq + q^2/2m,$$

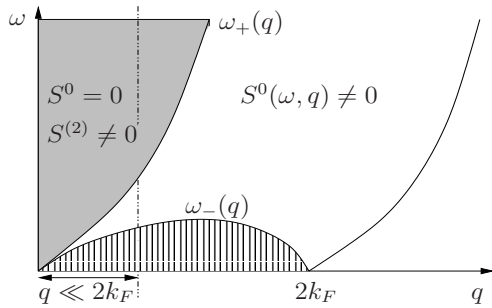


FIG. 1: The spectrum of excitations in a one-dimensional liquid of fermions.

*cf.* Fig. 1 with an additional broadening of the order of  $Tq/mv$  at non-zero temperatures (temperature overwhelms quantum fluctuations for  $T \gg vq$ ). The DSF therefore consists of two boxes centered around the massless mass-shells:  $\omega = \pm vq$ , each box having a width  $\delta\omega = |\omega_+ - \omega_-| = q^2/m + Tq/mv$  (which corresponds to the decay rate of the plasmons or Luttinger bosons) and a height  $\pm m/2|q|$  (positive sign for right-movers and negative sign for left-movers), *cf.* Fig. 2.

More non-trivial effects on this box-like shape are expected from interactions among fermions. In particular, the authors of Ref. [5] have shown that long-range tails to the DSF develop in second order of perturbation theory in interactions beyond the  $|\omega_+|$ -line and have given an expression for the zero-temperature tail. In this rapid note, our goal will be mainly to re-derive their result by using diagrammatics which we think brings a different and interesting approach to the problem. We further apply our results to curvature corrections to the small- $q$ , high- $\omega$  conductivity and to the electron-electron scattering rate. The major difficulty arising from diagrammatics is that the interplay between curvature and interactions leads to the breakdown of the loop cancellation theorem, a substantial technical complication as diagrams beyond the RPA are generated.

The simplest model which captures the interplay between curvature and interactions is the one of spinless fermions interacting with the  $g_2$  process, *i.e.* right-moving (+) fermions scattering on left-moving (-) fermions and vice-versa. Within this model, curvature is fully taken into account while interactions are treated perturbatively<sup>9</sup>. In the second order 10 diagrams arise, *cf.* Fig. 3. These diagrams are well-known. Diagrams R1, R2, L1 and L2 correspond to the re-normalization of a particle line. Diagrams R3 and L3 to a vertex correction. Diagrams M1 and M2 (which appear with a factor of two) are known in the theory of superconductivity as the Aslamazov-Larkin diagrams. To the knowledge of

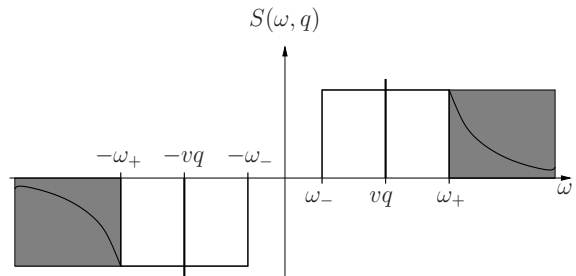


FIG. 2: The DSF,  $S(\omega, q)$ , as a function of frequency at a given momentum.

the author, these diagrams have not been computed for one-dimensional fermions with mass. In 3D, the first calculation was done by DuBois and Kivelson [10] and in 2D by Reizer and Vinokur [11]. As previously mentioned, in 1D, we are only aware of the results of Ref. [5] concerning the existence of tails beyond the  $|\omega_+|$ -line for the DSF.

We outline our main results leaving the proofs for a later publication [12]:

- 1) We consider first the case  $m \rightarrow \infty$ . From the loop cancellation theorem, the sum of all diagrams should be zero. We find that the combinations: R1+R2+R3, L1+L2+L3 and M1+M2, vanish in this limit. This implies that all R diagrams contribute equally, as well as all L diagrams and both M diagrams. Instead of working with individual diagrams we therefore work with the above combinations.
- 2) We consider then right- and left-movers with curved spectrum. Working with the combinations of diagrams defined in 1), which vanish in the case of a linear spectrum, we implement a systematic expansion in  $1/m$ . We prove that diagrams R1+R2+R3 have an expansion in  $1/m_+^2$ , diagrams L1+L2+L3 have an expansion in  $1/m_-^2$  and diagrams M1+M2 have an expansion in  $1/m_+m_-$  ( $m_+$  and  $m_-$  being the masses of right- and left-movers, respectively). This justifies the denomination of R and L diagrams as chiral diagrams and M diagrams as mixed diagrams (they mix the chiralities of the fermions).
- 3) We focus on the lowest order in the above  $1/m$  expansion. This amounts to focus on the tails of the DSF,  $|\omega| \gg vq$ . The arguments of 2) show that the tails provided by R (resp. L) diagrams correspond to the scattering of a curved right (resp. left) mover on a bosonized left (resp. right) mover (*i.e.* left (resp. right) mover with linear spectrum). On the other hand the tails of the mixed diagrams require the scattering of two curved fermions with different chiralities. This can be easily seen from

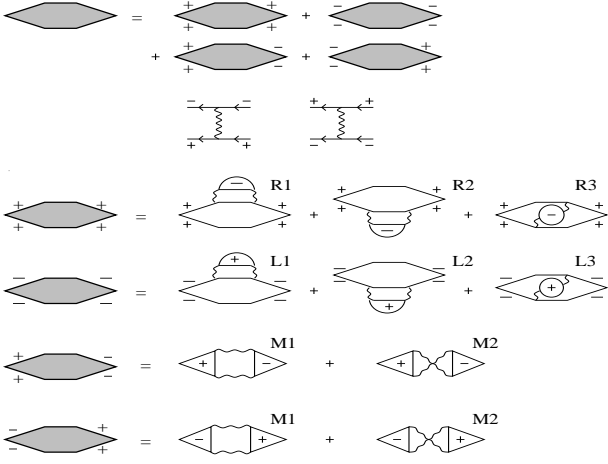


FIG. 3: The 2nd order contributions to the polarization operator of spinless fermions interacting with the  $g_2$  process, *i.e.* + fermions scattering on -fermions and vice-versa.

our general results which read:

$$\Im\Pi_R^{(2)R}(\omega, q) = -\frac{|V[\frac{\omega-vq}{2}]|^2}{256\pi v^5} \frac{q^2}{m_+^2} \frac{\omega+vk}{\omega-vq} \mathcal{F}(T; \omega, q) - \{\omega \rightarrow -\omega, \quad q \rightarrow -q\}, \quad (6a)$$

$$\Im\Pi_L^{(2)R}(\omega, q) = -\frac{|V[\frac{\omega+vk}{2}]|^2}{256\pi v^5} \frac{q^2}{m_-^2} \frac{\omega-vq}{\omega+vk} \mathcal{F}(T; \omega, q) - \{\omega \rightarrow -\omega, \quad q \rightarrow -q\}, \quad (6b)$$

$$\Im\Pi_M^{(2)R}(\omega, q) = +\frac{V[\frac{\omega+vk}{2}]V[\frac{\omega-vq}{2}]}{256\pi v^5} \frac{2q^2}{m_+m_-} \mathcal{F}(T; \omega, q) - \{\omega \rightarrow -\omega, \quad q \rightarrow -q\}, \quad (6c)$$

where  $\Im\Pi_\eta^{(2)R}(\omega, q)$  is the sum of all diagrams in the given class  $\eta = R, L, M$  and the temperature factor reads:

$$\mathcal{F}(T; \omega, q) = \frac{1}{1 - e^{-\frac{\omega-vq}{2T}}} - \frac{1}{1 - e^{-\frac{\omega+vk}{2T}}}. \quad (7)$$

4) We first comment on the effect of the long-range potential  $V[q]$ . As these expressions are valid for the tails of the correlation function,  $|\omega| \gg vk$ , the interaction potential factorizes and brings a contribution:  $|V[\omega/2]|^2$ . The three groups of diagrams (R, L and M) therefore cannot be discriminated by the inclusion of a long-range potential as far as the tails are concerned. Notice, however, that the long-range static Coulomb interaction acquires a dynamical nature depending on the external frequency,  $\omega$ . This dependence provides further  $\omega$ -tails to the dynamical structure factor. Actually, for a realistic three-dimensional Coulomb interaction we have:  $V(q) = -e^2 \ln(|q|a)$ , where  $a$  is a short distance cut-off. Therefore, the long-range 3D Coulomb potential provides an additional frequency dependence:  $|V[\omega/2]|^2 = e^4 \ln^2(|\omega|a/2v)$ , which is marginal.

5) Next we comment on the effect of temperature. Notice that the temperature factor of Eq. (7) is common

to all diagrams and therefore disables any discrimination between them. It has the following limiting expressions:

$$\mathcal{F}_0 = \Theta[\omega - vk] - \Theta[-\omega - vk], \quad |\omega \pm vk| \gg T, \quad (8a)$$

$$\mathcal{F}_\infty = \frac{4T\omega}{\omega^2 - (vk)^2}, \quad |\omega \pm vk| \ll T. \quad (8b)$$

We see clearly from the zero-temperature result of Eq. (8a) that the tails are restricted to the regions  $|\omega| \gg vk$ , *i.e.* beyond the  $|\omega_+|$ -line in agreement with Ref. [5]. For  $T \gg |\omega|$ , the tails acquire a linear  $T$ -dependence, *cf.* Eq. (8b).

6) We focus on the specific case of zero-temperature. In the following we assume that  $m_+ = m_- = m$ . We also consider a point-like interaction,  $V[q] = V_0$ , even though all results may be generalized to the case of a long-range interaction by changing:  $V_0 \rightarrow V[\omega/2]$ . We find that, as far as the tails of the DSF are concerned, all groups of diagrams contribute equally to the correlation function:

$$S^{(2)}(\omega, q) = -\Im\Pi_R^{(2)R}(\omega, q) - \Im\Pi_L^{(2)R}(\omega, q) - \Im\Pi_M^{(2)R}(\omega, q), \quad (9)$$

which reads:

$$S^{(2)}(\omega, q) = \frac{V_0^2}{64\pi v^3} \left(\frac{q^2}{m}\right)^2 \frac{1}{\omega^2 - (vk)^2} \mathcal{F}_0 - \{\omega \rightarrow -\omega, \quad q \rightarrow -q\}, \quad T \ll |\omega|, \quad (10)$$

where  $\mathcal{F}_0$  is given by Eq. (8a). Eq. (10) agrees with the result of Ref. [5].

7) We focus now on finite temperatures, *i.e.* for  $T \gg |\omega|$  (we still have  $|\omega| \gg vk$ ). Proceeding along the lines of the zero-temperature case yields:

$$S^{(2)}(\omega, q) = \frac{V_0^2}{16\pi v^3} \left(\frac{q^2}{m}\right)^2 \frac{\omega T}{(\omega^2 - (vk)^2)^2} - \{\omega \rightarrow -\omega, \quad q \rightarrow -q\}, \quad T \gg |\omega|, \quad (11)$$

which satisfies Eq. (5). Temperature therefore gives rises to frequency-tails proportional to  $T/\omega^3$  for a point-like interaction.

8) A general equation which interpolates between Eq. (10) and Eq. (11) reads:

$$S^{(2)}(\omega, q) = \frac{V_0^2}{64\pi v^3} \left(\frac{q^2}{m}\right)^2 \frac{1}{\omega^2 - (vk)^2} \mathcal{F}(T; \omega, q) - \{\omega \rightarrow -\omega, \quad q \rightarrow -q\}, \quad (12)$$

where the temperature factor is given by Eq. (7).

As a first application we determine the interaction correction to the tails of the conductivity beyond the TL approximation. The latter is defined as:

$$\Re\sigma(\omega, q) = e^2 \frac{\omega}{q^2} S(\omega, q). \quad (13)$$

In the absence of curvature Eq. (3) shows that the conductivity consists of delta peaks (Drude peaks) at the

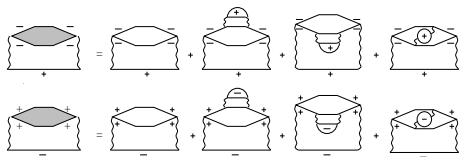


FIG. 4: Self-energy diagrams for spinless fermions interacting with the  $g_2$  process, *i.e.* + fermions scattering on -fermions and vice-versa.

mass-shells  $\omega = \pm vq$ . Including curvature from Eq. (4b), still in the absence of interactions, cures these mass-shell singularities yielding:

$$\Re\sigma^0(\omega, q) = \frac{e^2 v}{2} \frac{\omega \tau_q}{vq} \Theta[|\omega - vq| - q^2/2m], \quad (14)$$

where  $\tau_q = m/q^2$  is the decay-time of the Luttinger bosons. Including interactions, our previous results yield the interaction-correction to the high-frequency ( $|\omega| \gg vq$ ) small-momentum ( $q \ll 2k_F$ ) conductivity:

$$\Re\sigma^{(2)}(\omega, q) = \frac{e^2 V_0^2}{64\pi v^3} \frac{q^2}{m^2} \frac{\omega}{\omega^2 - (vq)^2} \mathcal{F}(T; \omega, q) - \{\omega \rightarrow -\omega, \quad q \rightarrow -q\}. \quad (15)$$

The  $\omega$ -tails are  $\propto 1/\omega$  for  $\omega \gg T$  and  $\propto T/\omega^2$  for  $\omega \ll T$ .

As a second application, we determine curvature corrections to the electron-electron scattering rate. It corresponds to the imaginary part of the self-energy diagrams represented on Fig. (4) on the Fermi shell,  $\tau_{\pm}^{-1}(\epsilon) \equiv \Im\Sigma_{\pm\mp}(\epsilon, k=0)$ . Notice that, because it is a single-particle property, the scattering rate does not depend on the mixed component of the polarization part. The 2nd order self-energy parts are well-defined in the massless

case and yield:  $\tau_{\pm}^{(2)}(\epsilon)^{-1} = -(V_0/v)^2 \max\{|\epsilon|, 2T\}$ , for a point-like interaction. The linear dependence on energy is known, *e.g.* see Ref. [13] for a review on the Luttinger liquid. From Eqs. (6a) and (6b) we may now access corrections to this scattering rate which go beyond the TL approximation. These are fourth-order corrections in interaction and second-order in mass. They yield the following energy-scale:

$$\tau^{(4)}(\epsilon)^{-1} = -\mathcal{N} \frac{V_0^4}{v^4} \frac{T^3}{\epsilon_F^2}, \quad (16)$$

where  $\mathcal{N} = \pi$  for  $\epsilon \ll 4T$  and  $\pi^2$  for  $\epsilon \gg 4T$ . This result is correct up to the fact that we know only the tails of the DSF. Interestingly enough, such a correction arises from 3-body processes among the interacting fermions<sup>14</sup> (recently, relaxation phenomena in disordered wires were shown to require 3 bodies (2 electrons and 1 impurity) [15]). Diagrammatically, this can be understood by the fact that the 4th order diagrams of Fig. (4) contain a cut with 5 particle-lines.

As a conclusion, we hope that our efforts to analytically derive curvature-corrections to the polarization operator and self-energy diagrams, through diagrammatics and in the case of spinless fermions, may motivate further work in understanding curvature effects in general and, possibly, relaxation processes in clean quantum wires.

Acknowledgements: I would like to thank I. Gornyi, I. Lerner, A. Mirlin, M. Pustilnik, and I. Yurkevich for discussions and particularly V. Kravtsov, and O. Yevtushenko with whom I have shared all progresses of the work, benefiting from their advice. I am indebted to L. Glazman for pointing the problem of the DSF tails and sharing his knowledge on it and D. Maslov for discussions on dephasing.

\* Electronic address: steber@ictp.trieste.it

<sup>1</sup> I. E. Dzyaloshinskii and A. I. Larkin, Sov. Phys.-JETP, **38**, 202 (1974).

<sup>2</sup> S. Brazovskii, S. Matveenko and P. Nozieres, J. Phys. I France, **4** 571 (1994).

<sup>3</sup> P. Kopietz and G. E. Castilla, Phys. Rev. Lett. **76**, 4777-4780, (1996).

<sup>4</sup> K. V. Samokhin, J. Phys.: Condens. Matter, **10** L533-L538 (1998).

<sup>5</sup> M. Pustilnik, E. G. Mishchenko, L. I. Glazman, and A. V. Andreev, Phys. Rev. Lett. **91**, 126805 (2003).

<sup>6</sup> A. V. Rozhkov, Eur. Phys. J. B, **47**, 193 (2005).

<sup>7</sup> A. G. Abanov and P. B. Wiegmann, Phys. Rev. Lett. **95**, 076402 (2005).

<sup>8</sup> A. A. Abrikosov, L. P. Gorkov and L. E. Dzyaloshinskii, "Methods of Quantum Field Theory in Statistical Physics", Dover Publications; Rev. English edition (June, 1977).

<sup>9</sup> Attempt to add curvature starting from bosonization is ill-defined, *i.e.* dealing perturbatively in  $m^{-1}$  with a Luttinger boson action:  $S[\varphi] = \dot{\varphi}^2 - (\partial_x \varphi)^2 - m^{-1}(\partial_x \varphi)^3$ .

This is because the perturbation theory is highly singular (singularity of the  $\delta(0)$  type) on the mass-shell of the non-interacting bosons  $\omega = \pm q$ . We were unable to resolve this singular perturbation theory (even for the free-fermion case). We therefore considered mass non-perturbatively and then the effect of interactions order by order.

<sup>10</sup> D. F. DuBois, M. G. Kivelson, Phys. Rev. **186**, 409 (1969).

<sup>11</sup> M. Yu. Reizer and V. M. Vinokur, Phys. Rev. B **62**, R16 306 (2000); E. G. Mishchenko, M. Yu. Reizer and L. I. Glazman, Phys. Rev. B **69**, 195302 (2004).

<sup>12</sup> S. Teber, details of the calculations.

<sup>13</sup> D. Maslov in Les Houches Summer School LXXXI, Elsevier Science (2005), H. Bouchiat et al. Editors.

<sup>14</sup> We could show, with the help of the Keldysh technique, that the fourth order self-energy diagrams of Fig. (4) give rise to a 6-fermion-occupation-function structure to the quantum kinetic equation [12].

<sup>15</sup> I. V. Gornyi, A. D. Mirlin and D. G. Polyakov, Phys. Rev. Lett. **95**, 046404 (2005).